Titre: Title:	Characterization of coarse mine waste rockfill using AI-assisted pressuremeter testing, large triaxial testing and CPTu
Auteurs: Authors:	Rafael Martínez, Gustavo Donoso, & Carlos Ovalle
Date:	2026
Type:	Article de revue / Article
Référence: Citation:	Martínez, R., Donoso, G., & Ovalle, C. (2026). Characterization of coarse mine waste rockfill using AI-assisted pressuremeter testing, large triaxial testing and CPTu. EPJ Web of Conferences, 385, 02003 (11 pages). Présentée à 1st Scientific Colloquium - Large Scale Testing (LST 2026), Karlsruhe, Germany. https://doi.org/10.1051/epjconf/202638502003

Titre de la revue: Journal Title:	EPJ Web of Conferences (vol. 385)
Maison d'édition: Publisher:	EDP Sciences
URL officiel: Official URL:	https://doi.org/10.1051/epjconf/202638502003

Characterization of coarse mine waste rockfill using AI-assisted pressuremeter testing, large triaxial testing and CPTu

Rafael Martínez[1*], *Gustavo* Donoso[2], and *Carlos* Ovalle[3]

[1]Pangea Geotecnia, Chile
[2]BHP, Chile
[3]Polytechnique Montreal, Canada

Abstract. The mining industry must address a wide range of geotechnical problems, many of which involve coarse materials and large particles, including heap-leach piles, spent-ore dumps, run-of-mine (ROM) piles, open pits, and foundation materials. Over the years, the industry has relied on large-scale laboratory testing, geophysics, and in situ testing. However, no single method appears to consistently dominate practice, as CPTu does for tailings. Pressuremeters can test a large volume of material and have been used worldwide for more than 70 years. Nevertheless, their full potential has been limited by traditional interpretation methods. Today, this limitation can be overcome with advanced numerical modelling and artificial intelligence. This paper presents the use of pressuremeter tests to characterise a 40 m-high spent-ore dump in northern Chile. The tests are back-analysed using advanced constitutive models and an AI-assisted software tool (DAARWIN) to match numerical predictions to measured responses. The resulting material parameters are then used to model the structure, and the predictions are compared with field-monitoring data and the results of CPTu and triaxial tests.

1 Introduction

The pressuremeter was developed by Ménard in the 1950s and was later refined at the University of Cambridge in the 1970s through the introduction of strain gauges to measure displacement (Lopes, 2022). The instrument measures the applied pressure and the corresponding cavity displacement at any depth within a borehole. The measured pressure-versus-cavity-displacement curve has been the subject of many studies as it is not a straightforward interpretation. In the authors' opinion, the difficulty of interpreting this curve has been the main obstacle to the instrument's wider use. Nowadays, fast computers and user-friendly finite-element software can model the test, and AI-based

* Corresponding author: rafael.martinez@pangeageotecnia.com

inverse analysis can iteratively adjust soil properties until the computed curve matches the measured curve (Martínez and Jara, 2024; Martínez et al., 2025).

For materials containing coarse particles, the pressuremeter offers a significant advantage because it mobilises a large volume of material. For a 70 mm-diameter instrument, the equivalent diameter of the mobilised zone is approximately 20 times larger, i.e., 1400 mm (Hughes and Whittle, 2022; Schnaid, 1990). Furthermore, considering the most recent soil-specimen-diameter-to-maximum-particle-size ratios reported in the literature (Girumugisha et al., 2024; Cantor and Ovalle, 2025), a ratio of around 15 should be adopted. Extending this assumption to the current study, it is assumed that a 70 mm-diameter pressuremeter can test materials containing particles up to approximately 1400/15 = 93 mm in diameter.

This paper describes site investigations undertaken following instability events in a 40 m-high spent-ore dump at a copper-mining operation in northern Chile. The material is classified as clayey gravel, with a maximum particle size of 30 mm. Triaxial tests on 300 mm × 150 mm (H x D) specimens and CPTu tests were conducted in 2022 as part of a campaign to investigate slope-instability events that occurred in 2021; however, the results proved inconclusive. In January 2026, pressuremeter tests were conducted to improve the characterisation of the material. The pressuremeter curves were interpreted by modelling the tests with an axisymmetric mesh in PLAXIS 2D using the Clay and Sand Model (CASM, Yu, 1998). The soil parameters were iterated using an artificial-intelligence code based on a genetic algorithm to minimise the root-mean-square difference between the modelled and measured responses (DAARWIN). The results show that the parameters obtained using this approach provide a substantially better representation of the deposit and allow cementation and partial-drainage effects to be addressed.

2 Site description

The spent-ore dump has a maximum height of approximately 40 m and a design slope angle of 30°. According to the USCS, the material classifies as clayey gravel (GC), with a maximum particle size of 30 mm and a fines content of approximately 27%, see Figure 1. The material is transported from a dynamic-leaching pile and deposited in a loose state by bucket-wheel excavators at a water content of 12% and a dry unit weight of γ_d = 14.4 kN/m³, corresponding to 68% of its Modified Proctor maximum dry density. This water content generates perched water tables, partial saturation and an irregular phreatic level, as indicated by the highly variable piezometric measurements recorded throughout the pile. The measured levels range from 10 to 30 m below ground surface.
From January to March 2021, several cracks appeared along the slope crests at the northern edge of the dump, accompanied by settlements of approximately 120 mm. Figure 2 shows a photograph of a crack (left) and survey measurements from the same date (right). The apparent failure-surface angle is approximately 39°, which differs considerably from the design slope angle of 30°.

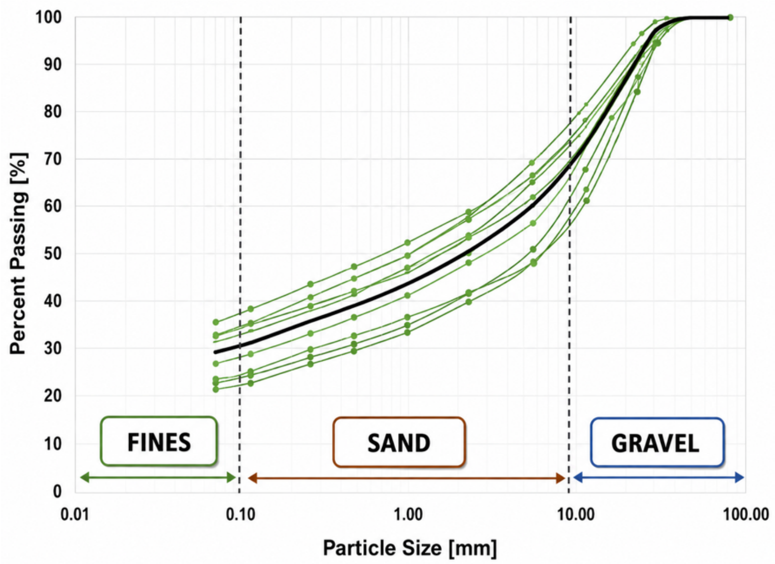

Fig. 1. Particle size distribution from trial pits.

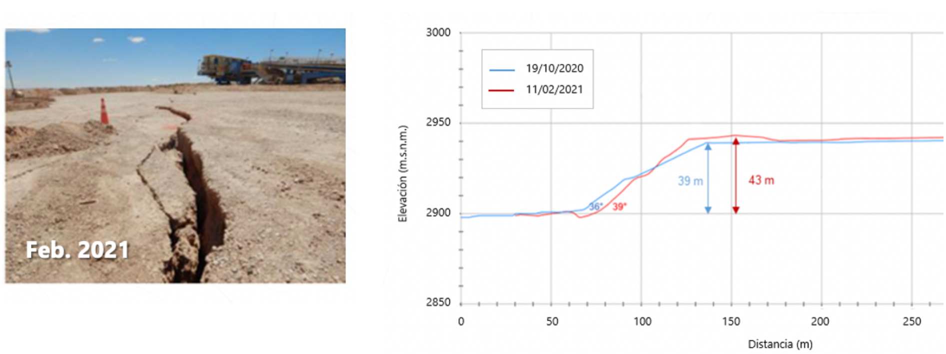

Fig. 2. Cracks (left) and survey results (right), February 2021.

3 Site investigations from 2022

Following the instability events observed in 2021, a comprehensive site investigation program was undertaken in 2022, comprising 12 sonic boreholes, 15 trial pits, and 12 CPTu tests. Laboratory testing included CIU and CID triaxial tests conducted on reconstituted specimens measuring 300 mm × 150 mm (H x D). The tested material was derived from bulk samples and core recovered from sonic drilling intervals using a 4¾-inch diameter sampler. The main results of this investigation are summarised below. The boreholes and CPTu results which will be analysed in this article are presented in Figure 3. It is seen their location is separated by less than 100m.

Fig. 3. Location of boreholes and CPTU analysed in this article.

3.1 Triaxial tests

Figure 4 presents the stress-strain curves and stress paths of the eight triaxial tests carried-out (4 CIU and 4 CID); Table 1 includes the confining pressures and the initial void ratios for all the tests.

The four sets of CID tests gave an average critical-state friction angle of φ'_{cs} = 29.1°, with a standard deviation of 4.1°. The four sets of CIU tests gave φ'_{cs} = 47.9°, with a standard deviation of 8.2°. Thus, the results are highly variable and do not exhibit a clear trend. Although disappointing, this outcome is not unexpected, as the specimen-diameter-to-maximum-particle-size ratio was $D/d_{\max} = 5$, below the minimum value of 6 required by the testing standard ASTM D7181, and well below the value of 15 recommended by recent studies on rockfill materials (Cantor and Ovalle, 2025; Girumugisha et al., 2024).

Table 1. Summary of the triaxial testing program. The test ID indicates the test type (CID or CIU), borehole number (03 or 07), and the depth interval of the sampled material in the borehole (e.g., 21.5–28 m).

Test ID	Initial confining pressure (kPa)	Initial void ratio
Tx-CIU-BO-03 21.5-28.0	100	0.492
	200	0.471
	400	0.459
Tx-CIU-BO-03 21.5-28.0	100	0.431
	300	0.383
	700	0.354
Tx-CID -BO-03 15.5-20.0	100	0.439
	200	0.389
	800	0.334
Tx-CID -BO-03 15.5-20.0	100	0.326
	500	0.279
	900	0.235
Tx-CIU-BO-07 18.0-20.0	100	0.495
	200	0.461
	400	0.389
Tx-CIU-BO-07 26.0-30.0	100	0.331
	300	0.267

Test ID	Initial confining pressure (kPa)	Initial void ratio
	700	0.216
Tx-CID -BO-07 20.0-23.0	100	0.346
	500	0.289
	900	0.254
Tx-CID -BO-07 23.0-26.0	100	0.475
	200	0.451
	800	0.421

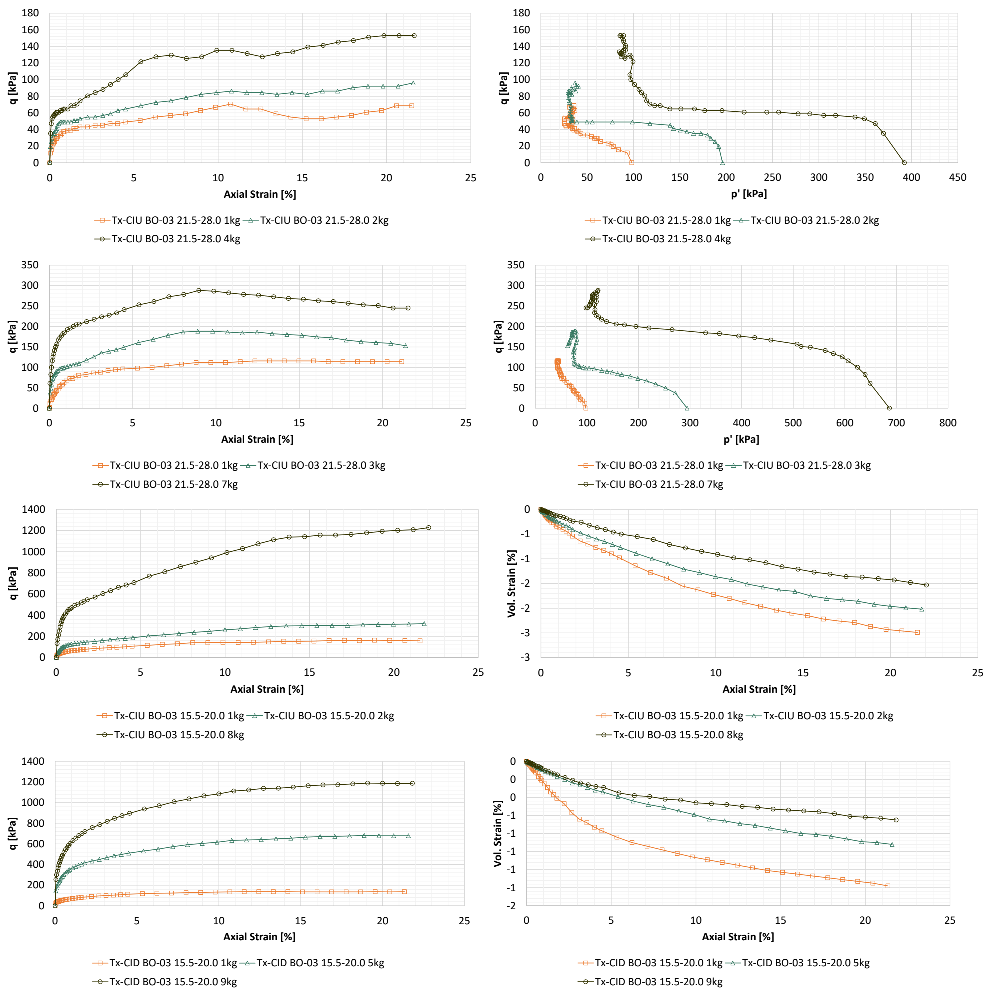

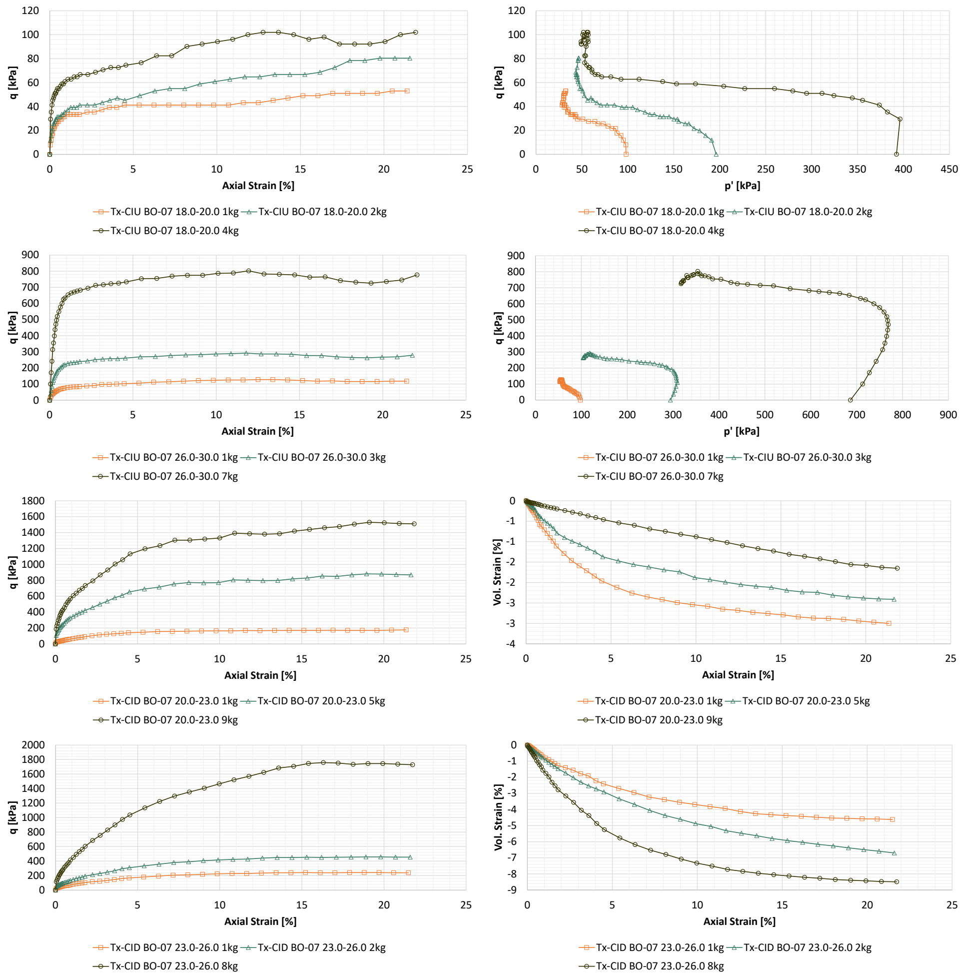

Fig. 4. Triaxial testing program comprising four sets of CIU tests and four sets of CID tests (three specimens per set), performed at confining pressures ranging from 100 to 900 kPa.

Figure 5 shows the range of E_{50} values obtained from the triaxial tests after substantial selective screening of the data. The results are compared with a large database reported by Ovalle et al. (2020), and lie close to its lower bound. The pressuremeter-derived values, discussed later in the paper, are also shown.

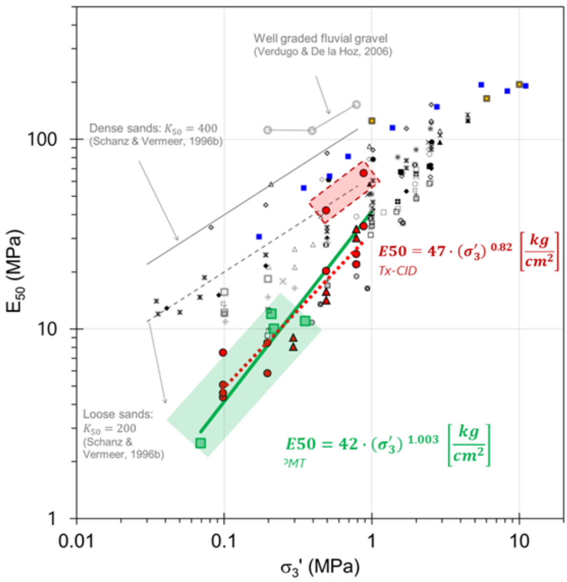

Fig. 5. E50 from triaxial and pressuremeter tests compared with an international database.

3.2 CPTu tests

The site-investigation campaign included 12 CPTu soundings at different locations. Six of these tests were concentrated along the failed zone, with distances of 60 to 300 m between test points. The sounding depths ranged from 19.7 to 43.7 m.

The soil-behaviour classification and qt-versus-depth plots for a representative CPTu profile are presented in Figure 6 (left and centre). The profile shows no laterally persistent stratigraphic units: features in the qt record do not correlate between soundings spaced 60–300 m apart, and the deposit was therefore treated as a single material in the analyses that follow. The qt trace is nevertheless highly variable, with excursions spanning approximately an order of magnitude over sub-metre intervals. Given a cone-diameter-to-maximum-particle-size ratio of about 1.0, this variability is attributed primarily to particle-scale interference rather than to layering. The Ic-based classification averages these excursions into an apparently uniform sandy silt to silty sand response (Ic ≈ 2.0–3.2) that gives no indication of the gravel fraction, despite its significant presence.

Characterising ageing and cementation is important when assessing the risks associated with these deposits. This analysis should preferably be based on the ratio of elastic stiffness to ultimate strength (G0/qc), following Eslaamizaad and Robertson (1997). Figure 6 (right) presents this analysis, with the current investigation shown as red dots. The results consistently plot above and outside the "normal" region, suggesting possible effects of stress history, cementation, and ageing. A sudden loss of this cementation during undrained loading could trigger strain-softening behaviour, as discussed below.

Figure 7 shows the u2 profiles (left) and the Bq calculations (centre). As recommended for low Bq values, a drained interpretation following Robertson and Campanella (1983) is also shown (right). Below 4m, most of the estimated friction angles are approximately 30°, which is inconsistent with the dump geometry and observed performance.

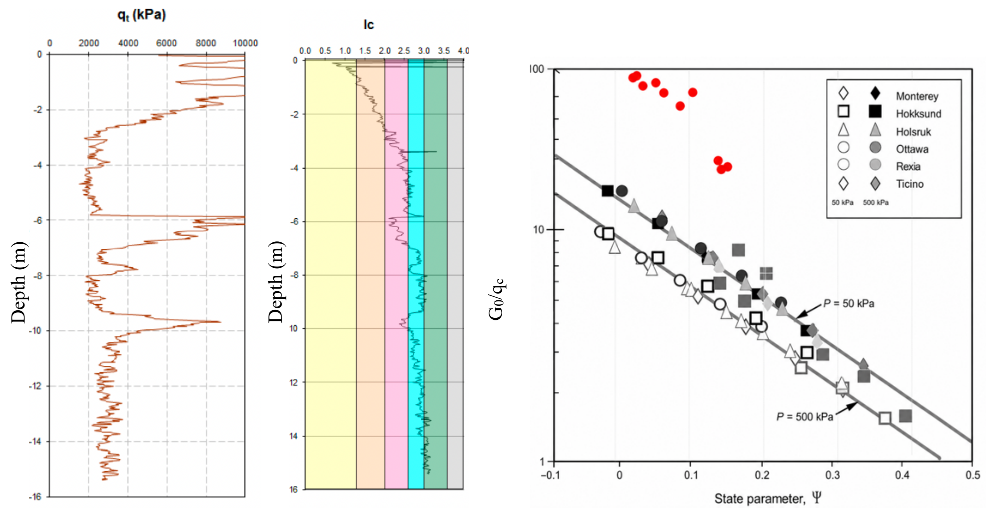

Fig. 6. A representative set of CPTu results.

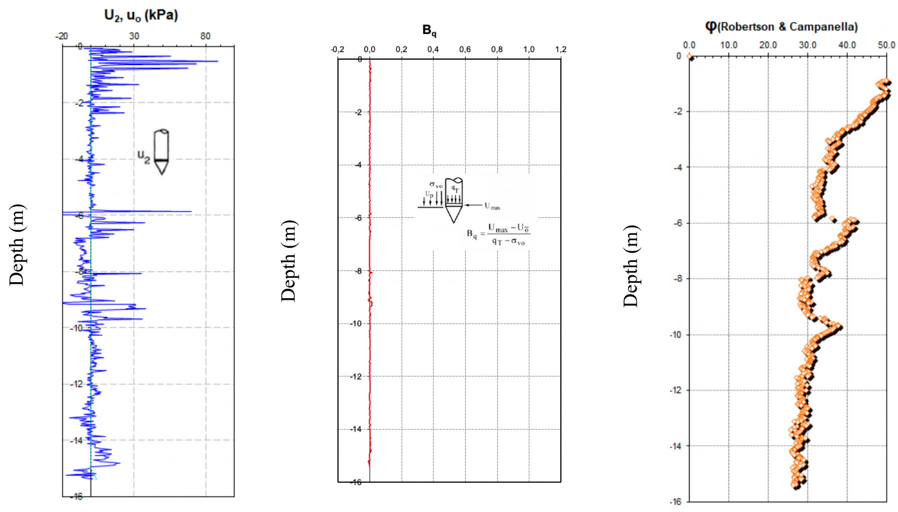

Fig. 7. u2, Bq, and strength estimates derived from CPTu.

Because similar results were consistently obtained from most of the other CPTu profiles, the applied correlation is believed not to adequately account for partial saturation and drainage, as reported by Holmsgaard et al. (2016).

4 Pressuremeter results

In December 2025 and January 2026, four 35 m-deep boreholes were drilled, and four pressuremeter tests were conducted in each borehole. A 70 mm-diameter OYO Elastmeter-3 was used. Figure 8 (left) shows four representative curves from one of the boreholes. The tests were modelled using an axisymmetric mesh in PLAXIS 2D, with the drained Clay and Sand Model (CASM; Yu, 1998) adopted to interpret the curves. This choice was based on the model's ability to use the state parameter (ψ_0) as an explicit variable and to represent strain-softening behaviour, which had been identified as a concern from the CPTu results shown in Figure 3 (right). To determine the best fit between the measured and modelled curves, the AI-assisted software DAARWIN, which uses a genetic algorithm, was applied as described by Martínez and Jara (2024) and Martínez et al. (2025). Figure 8 (right) shows the best fit obtained for one of the tests. Some of the best-fit parameters for CASM and the four tests are shown in Table 2.

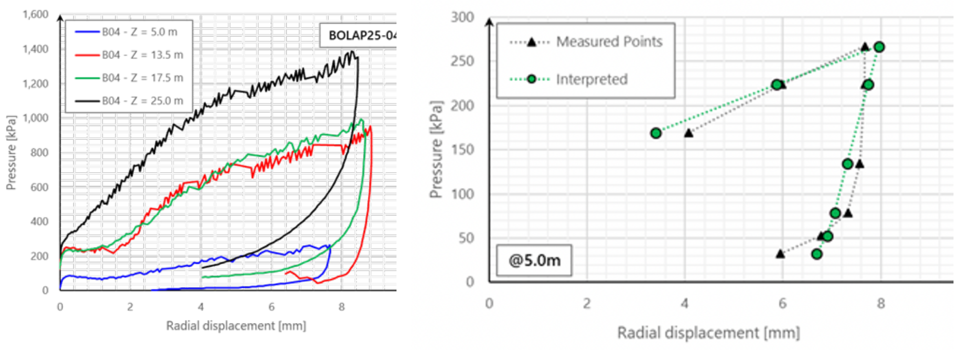

Fig. 8. PLAXIS model (left) and AI-assisted fit (right).

Table 2. **CASM parameters.**

Parameter	BO4–5 m	BO4–13.5 m	BO4–17.5 m	BO4–25 m
State Parameter (ψo)	0.132	0.110	-0.003	-0.012
Slope of the compression (λ)	0.0825	0.0630	0.0798	0.1078
Slope of the swelling (κ)	0.020	0.018	0.016	0.010
Friction angle at CS (ϕ_{cs})	39	39	40	39
Earth pressure at rest (K_0)	0.80	1.01	0.61	0.77

The consistency of the derived internal friction angles is noteworthy. Values of ϕ_{cs} = 39° to 40° are considered considerably more realistic, given the material gradation and the observed failure-surface angle of approximately 39°. The E50 values also fall within the range estimated from the triaxial tests, as shown in Figure 5. The state parameter values vary from loose to medium dense, consistent with a material that is loosely placed and systematically densifying under self-weight.

It is important to note that all pressuremeter tests were interpreted as drained, primarily on the basis of the low Bq values obtained from the CPTu tests. Although a drained interpretation was considered inappropriate for the CPTu results, it provided a much more satisfactory interpretation of the pressuremeter tests. This difference may be explained by the much larger volume of material mobilised by the pressuremeter. Some excess pore pressure may be generated close to the expanding membrane, but it is likely

to dissipate into the surrounding material, making the assumption of negligible average excess pore pressure within the mobilised zone more reasonable.
The proposed approach allows the calibrated soil parameters to be used to model other loading scenarios, such as an undrained triaxial test, even though the parameters were derived from a drained test. In this case, the simulations consistently indicate strain-softening behaviour; the curves are not shown because of space limitations. Although CASM was not developed specifically for cemented materials and does not include cohesion as a model parameter, the simulations show a sudden loss of strength under undrained loading. This response is consistent with the G0/qc relationships discussed in relation to Figure 5, but it was not observed in the triaxial tests, possibly because cementation develops over time and is destroyed when the specimens are remoulded. Further research and testing are under way to better understand this phenomenon.

4.1 Angle of repose tests

Because of the substantial inconsistencies among the triaxial, CPTu, and pressuremeter results, ten angle-of-repose tests were conducted. The close relationship between the angle of repose and the critical-state friction angle has been widely reported. The tests gave an average angle of repose of approximately 41° with a standard deviation below 1°, which is highly consistent with the pressuremeter-derived values.

5 Conclusions

Pressuremeter tests have been used for many years, but the difficulty of interpreting their results has hindered their wider adoption. Today, fast computers and readily available finite-element software can overcome this limitation. The test can be modelled, and the soil parameters can be determined by matching the measured field curve to the numerical response. This approach allows the soil to be characterised and a constitutive model to be calibrated in a single process, which can be further accelerated using AI-assisted tools. The instrument is particularly well suited to materials containing large particles because it mobilises a large volume of material. A 70 mm-diameter instrument is estimated to mobilise a zone with an equivalent diameter of approximately 1400 mm. The suitability of the approach was demonstrated by characterising a 40 m-high spent-ore dump comprising clayey gravel with a maximum particle size of 30 mm. Despite the challenging cementation and partially drained conditions, the combined pressuremeter–FEM–AI method consistently produced coherent stiffness and strength parameters, which had not been achieved using conventional triaxial or CPTu testing. The CASM parameters calibrated from the pressuremeter tests also reproduced aspects of the cemented response that had been suggested by other methods but not adequately characterised.

References

1. ASTM D7181-20. Standard Test Method for Consolidated Drained Triaxial Compression Test for Soils. West Conshohocken: ASTM International; 2020.
2. Cantor, D., Ovalle, C. (2025): Sample size effects on the critical shear strength of granular materials with varied gradation and the role of column-like local structures. Géotechnique 75(1), pp. 29-40 https://doi.org/10.1680/jgeot.23.00032.
3. Eslaamizaad, S., and Robertson, P. K. 1996a. Seismic cone penetration test to identify cemented sands. In *Proceedings of the 49th Canadian Geotechnical Conference*, St. John's, N.L., 23–25 September 1996. Edited by J. I. Clark. Canadian Geotechnical Society, Richmond, B.C. pp. 352–360.
4. Girumugisha, G., Ovalle, C., Ouellet, S. (2024). Grading scalping and sample size effects on critical shear strength of mine waste rock through laboratory and in-situ testing. International Journal of Rock Mechanics and Mining Sciences 83, 105915 https://doi.org/10.1016/j.ijrmms.2024.105915.
5. Holmsgaard R., Nielsen B., Ibsen L. (2016). Interpretation of Cone Penetration Testing in Silty Soils Conducted under Partially Drained Conditions, J. Geotech. Geoenviron. Eng., 2016, 142(1). https://doi.org/10.1061/(ASCE)GT.1943-5606.0001386.
6. Hughes, J. P., & Whittle, R. R. (2022). High Resolution Pressuremeters and Geotechnical Engineering. CRC Press eBooks. https://doi.org/10.1201/9781003200680.
7. Lopes A. (2022). Louis Ménard and the pressuremeter test. Comité Francais de la Mécaniqe des Sols. Accesed on 27th Abril 2024. https://www.cfmssols.org/sites/default/files/timecapsule/2%20Pressiometre%20et%20 Menard/EN%20rapport%20pressiom%C3%A8tre%20M%C3%A9nard.pdf
8. Martínez R. & Jara M. The use of Artificial Intelligence, Finite Element Modelling and Pressuremeter tests for geotechnical characterisation. In: Proceedings of the 17th Pan-American Conference on Soil Mechanics and Geotechnical Engineering, La Serena, 2024.
9. Martínez R., Jara M., Schnaid F., Montava G. On the determination of the at-rest lateral earth pressure coefficient and the state parameter using pushed-in high-resolution Pressuremeters. In: Proceedings of the 8th International Symposiun on Pressuremeters, Luxembourg, 2025.
10. Ovalle, C., Linero, S., Dano, C., Bard, E., Hicher, P.-Y., Osses, R. (2020): Data compilation from large drained compression triaxial tests on coarse crushable rockfill materials. Journal of Geotechnical and Geoenvironmental Engineering 146(9): 06020013 https://doi.org/10.1061/(ASCE)GT.1943-5606.0002314.
11. Robertson, P.K. and Campanella, R.G., (1983). Interpretation of cone penetration tests. Part I: Sand. *Canadian Geotechnical Journal*, 20(4), pp.718–733. https://doi:10.1139/t83-078.
12. Schnaid F. "A study of the cone-pressuremeter test in sand", Phd thesis, University of Oxford, 1990.
13. Yu, H. S., 1998, CASM: A unified state parameter model for clay and sand. International Journal for Numerical and Analytical Methods in Geomechanics, 22(8), 621-653.